

Monolithically integrated optical modulator based on polycrystalline $\text{Ba}_{0.7}\text{Sr}_{0.3}\text{TiO}_3$ thin films

Zhimou Xu,^{a)} Masato Suzuki, Yuichiro Tanushi, and Shin Yokoyama^{b)}
*Research Center for Nanodevices and Systems, Hiroshima University, 1-4-2 Kagamiyama,
 Higashi-Hiroshima 739-8527, Japan*

(Received 18 November 2005; accepted 8 March 2006; published online 17 April 2006)

Good-quality polycrystalline $\text{Ba}_{0.7}\text{Sr}_{0.3}\text{TiO}_3$ (BST0.7) thin films were deposited on fused silica substrates and Si substrates having a thick amorphous SiO_2 layer at a relatively low temperature of 550 °C by spin-coating metal organic solutions. The thin films were highly transparent to light in the ultraviolet to near-infrared wavelength regions. The optical propagation loss for a 5- μm -wide and 300-nm-thick polycrystalline waveguide based on BST0.7 was about 17 dB/cm at a wavelength of 632.8 nm. An electro-optic Mach-Zehnder interferometer modulator based on the polycrystalline BST0.7 thin film was monolithically integrated on a Si substrate with standard lithography and wet etching. Optical modulation was successfully demonstrated. The estimated electro-optic coefficient (6.7 pm/V) is the highest reported so far for this kind of film deposited on a fused silica substrate or a Si substrate with an amorphous SiO_2 layer. © 2006 American Institute of Physics.

[DOI: 10.1063/1.2197288]

The electro-optic (EO) characteristics of ferroelectric thin films have been widely studied for use in EO switches, modulators, and optical waveguides in conventional hybrid optoelectronic integrated circuits (OEICs).^{1,2} Recently, $(\text{Ba}_x\text{Sr}_{1-x})\text{TiO}_3$ (BST) thin films have attracted attention due to their interesting EO characteristics.³ Despite the recent advances made in the fabrication and characterization of such ferroelectric thin films, little data about monolithic integration of ferroelectric thin-film EO switches, modulators, and optical waveguides on silicon substrates have been published. We previously reported the design concept of a Mach-Zehnder interferometer (MZI) switch and modulator based on highly (100)-oriented sputtered-BST thin films monolithically integrated on a Si substrate having a thick SiO_2 layer at 700 °C.⁴ However, 700 °C is too high for fabricating monolithically integrated optical interconnections in large scale integration (LSI) chips, usually the final process in fabricating OEICs. Generally, a lower fabrication temperature, for example, lower than 450 °C (Ref. 5) is essential in order to prevent damage to the LSI chips.

In this letter we demonstrate the successful operation of a monolithically integrated MZI optical modulator based on metal organic solution-derived polycrystalline $\text{Ba}_{0.7}\text{Sr}_{0.3}\text{TiO}_3$ (BST0.7) thin films deposited at a relatively low temperature of 550 °C. The estimated linear EO coefficient (6.7 pm/V) of this BST0.7 thin film is the highest reported so far for this kind of polycrystalline film deposited on a fused silica substrate or a Si substrate with an amorphous SiO_2 layer.

BST0.7 thin films were deposited on fused silica substrates and Si substrates having a SiO_2 thermal oxide layer with a thickness larger than 1.0 μm . The thin films were deposited by spin-coating metal organic solutions. A mixture of $\text{Ti}(\text{C}_4\text{H}_9\text{O})_4$, $\text{Sr}(\text{C}_8\text{H}_{15}\text{O}_2)_2$, $\text{Ba}(\text{C}_8\text{H}_{15}\text{O}_2)_2$, and $\text{CH}_3\text{COOC}_2\text{H}_4\text{CH}(\text{CH}_3)_2$ was used as the starting material. Their molar ratios were appropriately set to produce the de-

sired composition of BST0.7 (Ba:Sr:Ti=0.7:0.3:1). The precursor solution was spin coated at 500 rpm for 10 s, followed by 2000–2200 rpm for 20 s. Each wet layer was initially dried at 180 °C for 10 min to evaporate the solvent, and rapidly prebaked at 450 °C for 30 min on a hot plate in a clean room to remove residual organics. The desired thickness of the BST0.7 layer was achieved using multiple spin-coating and prebaking steps. Finally, the multilayer films of the desired thickness were annealed at different temperatures in open air in a conventional box furnace. The heating and cooling rates were kept at 5 and 3 °C/min, respectively. The structure of the BST0.7 thin films produced was analyzed by x-ray diffraction (XRD, Rigaku RINT2100) with a copper target. The thickness of the thin films was measured by a film thickness measurement system (Nanometrics, Nanospec/AFT 5000) and cross-sectional images of the samples with a field-emission scanning electron microscope (SEM, Hitachi S-4700). The surface morphology of the films was observed using an atomic force microscope (AFM, Seiko Instruments SPA3800). The surface root mean square (rms) roughness was evaluated from a 1 μm^2 area of the AFM image.

Figure 1 shows the XRD patterns of BST0.7 films with a thickness of about 200 nm after postannealing at different temperatures. The substrates were fused silica. The BST0.7 thin films became more crystalline, with the (110) orientation being dominant, as indicated by the relative intensities of the

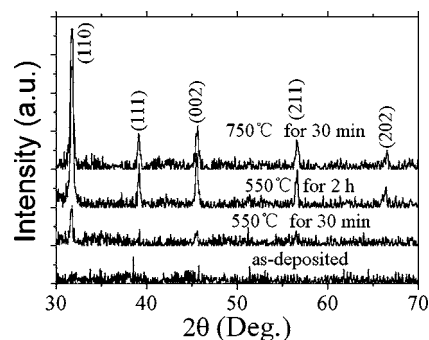


FIG. 1. XRD patterns of about 200-nm-thick BST0.7 films postannealed at different temperatures. The substrates were fused silica.

^{a)}On leave from Department of Optoelectronic Engineering, Huazhong University of Science and Technology, Wuhan 430074, People's Republic of China.

^{b)}Author to whom correspondence should be addressed; electronic mail: yokoyama@sxsys.hiroshima-u.ac.jp

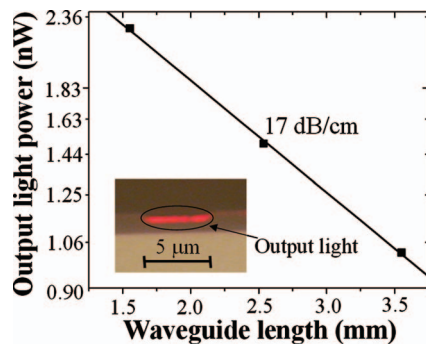


FIG. 2. (Color) Plot of output light power vs waveguide length of a groove-type planar optical waveguide and picture (inset) of the output light. The optical propagation loss is obtained from the slope of a fitted straight line.

XRD peaks in Fig. 1. No clear peaks attributed to crystalline BST0.7 appeared in the as-deposited films prebaked at 450 °C for 30 min, indicating the amorphous nature of the films. Crystallization begun to appear when the films were postannealed at 550 °C for 30 min. A perfect pseudocubic perovskite phase of BST0.7 had already formed at 550 °C after 2 h of postannealing. This complete crystallization temperature is about 100–200 °C lower than that reported in other studies using similar chemical solution-derived BST0.7 film-forming methods, such as sol-gel⁶ and metal organic deposition⁷ methods. One of the main reasons is the different precursor solution used in our experiments. The constituents of the precursor mixture easily reacted with each other and formed intermediate phases at a low fabrication temperature of about 337 °C according to XRD results and thermogravimetric and differential thermal analysis results (not shown, provided by Kojundo Chemical Laboratory Co. Ltd., Japan). The lower crystallization temperature is advantageous for monolithically integrating BST0.7-film waveguide devices in OEICs for optical interconnections. The thin films were highly transparent to light in the ultraviolet to near-infrared wavelength regions from 300 to 2400 nm (not shown). Considering the structure and lower fabrication temperature requirements for optical interconnections in LSI, the BST0.7 thin films postannealed at 550 °C for 2 h were selected for optical waveguide devices monolithically integrated in LSI chips.

To avoid the increased optical propagation loss α_L associated with etching polycrystalline BST0.7 thin films in a thin-film waveguide monolithically integrated on Si, a groove-type planar optical waveguide with a BST0.7-based core layer was fabricated without etching. First, 5- μm -wide and 700-nm-deep SiO_2 groove patterns were fabricated on a Si substrate with a 1.65 μm SiO_2 thermal oxide layer by electron beam lithography and reactive ion etching. Second, BST0.7 thin films were deposited on the groove substrate by the spin-coating procedure described above. The BST0.7 core formed in the groove was 5 μm wide and 300 nm thick. The thin film formed outside the groove was about 240 nm thick. Finally, without etching, postannealing at 550 °C was performed for 2 h to complete the groove-type planar optical waveguide. The propagation loss α_L was evaluated using an experimental setup similar to that reported by Petraru *et al.*² To perform cutback measurement, waveguides of different lengths were prepared and the transmission of 632.8 nm light through the waveguide was measured. From the transmission of the waveguides, α_L was determined to be about 17 dB/cm at this wavelength (Fig. 2). An image of the output light from

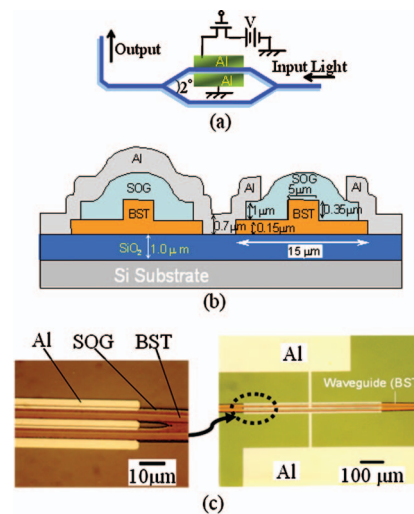


FIG. 3. (Color) Schematic top view (a), cross-sectional view (b), and photomicrographs (c) of a MZI modulator monolithically integrated on Si. Channel waveguides with a width of 5 μm and a step height of about 350 nm were patterned on a 500-nm-thick polycrystalline BST0.7 thin film using standard optical lithography and wet etching.

the groove-type planar optical waveguide is shown in the inset of Fig. 2. It was found that most light was confined in the polycrystalline BST0.7 core layer in the groove. This value of optical propagation loss is acceptable for high-index-contrast waveguides, for example, low-loss polycrystalline silicon waveguides (35 dB/cm at a wavelength of 1.55 μm),⁸ because the total length of optical waveguides in LSI chips is typically only a few centimeters. The optical propagation loss is mainly ascribed to optical releases in the BST0.7 thin films formed outside the groove. In addition, optical propagation losses in the waveguide are caused by surface scattering due to surface roughness. The rms roughness of the polycrystalline BST0.7 film was about 2.7 nm. A further reduction in optical loss is expected with suitable design of the waveguide structure, for example, using a ridge waveguide,² and improvement of the rms roughness by careful handling of the solution and substrate and careful control of the deposition conditions.

Channel waveguides with a width of 5 μm and a step height of about 350 nm were patterned on a 500-nm-thick polycrystalline BST0.7 thin film using standard optical lithography and wet etching to form a MZI modulator monolithically integrated on Si, as shown in Fig. 3. The top and bottom cladding layers were, respectively, a spin on glass (SOG) and a SiO_2 thermal oxide layer with a thickness of 1 μm . The polycrystalline BST0.7 thin film waveguides were patterned after being etched for about 30 s with a BHF solution (BHF:H₂O=1:9). Al electrodes with a length of 600 μm and a separation of 15 μm were then deposited. The input and output faces of the modulator were then cleaved. In-plane polarized light was supplied from a He-Ne laser (wavelength of 632.8 nm) and was end-fire coupled into the waveguide. The output light was coupled to a solid-state photodetector (Newport, model 818-SL). We observed the modulation behavior of the MZI modulator at 632.8 nm by measuring the output intensity versus the applied voltage, as shown in Fig. 4. The voltage was applied to one arm of the MZI modulator. The instability of the output from the He-Ne laser and noise from the modulator were smaller than the modulation amplitude. The change in output intensity ΔI

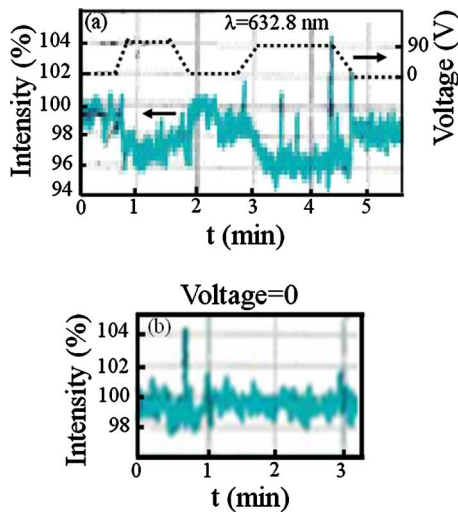


FIG. 4. (Color online) Optical response of the MZI modulator monolithically integrated on Si while the applied voltage was changed (a) and when equal to 0 V (b) at a wavelength of 632.8 nm. The voltage was applied to one arm of the modulator.

caused by the linear EO effect of the MZI modulator can be described by⁹

$$\Delta I = \frac{I}{I_0} = \frac{1 + \cos(\Delta\varphi)}{2}, \quad (1)$$

where I and I_0 are the intensities of the output light from the MZI modulator with and without an applied bias voltage, respectively. $\Delta\varphi$ is the optical phase shift in the MZI modulator, which is given by

$$\Delta\varphi = 2\pi \frac{\Gamma(1/2)r_{\text{eff}}^3 n_e^3 (V/G)l}{\lambda},$$

where r_{eff} is the effective EO coefficient of the core layer, n_e is the effective refractive index of the core layer, V is the applied voltage, G is the gap between the two electrodes, l is the length of one arm of the MZI modulator, λ is the measurement light wavelength, and Γ is the reduction factor of the applied electric field. Γ is simulated as 0.22, where the relative dielectric constant of BST0.7 is about 160.^{9,10}

Substituting ΔI into Eq. (1), it is found that an optical phase shift of 16.2° is realized in a MZI modulator with 600- μm -long arms when the applied dc voltage is 90 V. It is therefore expected that a much larger optical phase shift will be obtained by increasing the arm length of the MZI modulator. Assuming the value $n_e=2.2$,¹¹ respectively, the r_{eff} of the polycrystalline BST0.7 thin film estimated from the MZI optical response is about 6.7 pm/V, which is about 1/5 of that of bulk LiNbO₃ ($r_{33}=30$ pm/V) and polycrystalline BaTiO₃ deposited on MgO by pulse laser deposition techniques ($r_{\text{eff}}=22$ pm/V).² This can be compared to the results obtained by Gia Russo and Kumar¹² for polycrystalline LiTaO₃ films ($r_{\text{eff}}=0.32$ pm/V) and Griffel *et al.*¹³ for polycrystalline LiNbO₃ ($r_{\text{eff}}=1.34$ pm/V) sputtered on fused silica substrates.

The EO effect may be related to the crystalline quality of ferroelectric thin films.¹² Single-crystal bulk material and epitaxial or high-crystallinity ferroelectric films deposited on single-crystal nonsilicon substrates have much larger EO coefficients because of their much higher crystallinity than nor-

mal polycrystalline films. Depositing high crystallinity films on fused silica substrates and Si substrates with an amorphous SiO₂ layer is very challenging, especially at low fabrication temperatures. The films deposited in this way appear to be either amorphous or normally polycrystalline^{2,12,13} and show very low EO efficiency.^{12,13} In our experiments, we obtained good-quality BST0.7 polycrystalline films deposited on fused silica substrates and Si substrates with thick amorphous SiO₂ layers at a lower fabrication temperature of 550 °C. The polycrystalline films we fabricated have the highest linear EO coefficient reported so far for this kind of film.^{12,13} However, the crystalline quality is lower than that of single-crystal bulk material and epitaxial or high-crystallinity ferroelectric films deposited on single-crystal nonsilicon substrates. Future work in this direction is to improve the crystalline quality and EO effect of the MZI at lower fabrication temperatures. Although the modulation efficiency obtained in this study is not large, we nevertheless demonstrated successful optical modulation using a monolithically integrated electro-optical device based on a polycrystalline BST0.7 thin film. Their EO response characteristics make polycrystalline ferroelectric thin films attractive for EO thin-film waveguide devices monolithically integrated with LSI technology, replacing some of the existing hybrid devices made from single crystals, bulk polycrystalline materials, and epitaxial or highly crystalline thin films deposited on single-crystal nonsilicon substrates.

In conclusion, good-quality transparent polycrystalline BST0.7 films were grown on fused silica substrates and Si substrates at a relatively low temperature by spin-coating metal organic solutions. The films have useful EO properties. A MZI optical modulator monolithically integrated on a Si substrate was demonstrated. This device was estimated to have an effective EO coefficient of $r_{\text{eff}}=6.7$ pm/V.

This study was supported in part by the 21st Century COE program “Nanoelectronics for Tera-Bit Information Processing” and a Grant-in-Aid for Scientific Research (B) (17360166, 2005) from the Ministry of Education, Culture, Sports, Science and Technology of Japan.

¹S.-H. Lee, T. W. Noh, and J.-H. Lee, Appl. Phys. Lett. **68**, 472 (1996).

²A. Petraru, J. Schubert, M. Schmid, O. Trithaveesak, and Ch. Buchal, Opt. Lett. **28**, 2527 (2003).

³D. Kim, S. Moon, E. Kim, S. Lee, J. Choi, and H. Kim, Appl. Phys. Lett. **82**, 1445 (2003).

⁴Z. M. Xu, M. Suzuki, and S. Yokoyama, Jpn. J. Appl. Phys., Part 1 **44**, 8507 (2005).

⁵C. Y. Chang and S. M. Sze, *ULSI Technology* (McGraw-Hill, New York, 1996), p. 424.

⁶X. F. Chen, W. Q. Lu, W. G. Zhu, S. Y. Lim, and S. A. Akbar, Surf. Coat. Technol. **167**, 203 (2003).

⁷S. Y. Chen, H. W. Wang, and L. C. Huang, Mater. Chem. Phys. **77**, 632 (2002).

⁸J. S. Foresi, M. R. Black, A. M. Agarwal, and L. C. Kimerling, Appl. Phys. Lett. **68**, 2052 (1996).

⁹H. Nishihara, M. Haruna, and T. Suhara, *Optical Integrated Circuits* (McGraw-Hill, New York, 1989), p. 286.

¹⁰H. Zhu, J. Miao, M. Noda, and M. Okuyama, Sens. Actuators, A **110**, 371 (2004).

¹¹B. Panda, A. Dhar, G. D. Nigam, D. Bhattacharya, and S. K. Ray, Thin Solid Films **332**, 46 (1998).

¹²P. P. Gia Russo and C. S. Kumar, Appl. Phys. Lett. **23**, 229 (1973).

¹³G. Griffel, S. Ruschin, and N. Croitoru, Appl. Phys. Lett. **54**, 1385 (1989).